NASA Technical Memorandum 100116

Measured Performance of the Heat Exchanger in the NASA Icing Research Tunnel Under Severe Icing and Dry Air Conditions

W. Olsen, J. Van Fossen, and R. Nussle
Lewis Research Center
Cleveland, Ohio

December 1987

NASA

MEASURED PERFORMANCE OF THE HEAT EXCHANGER IN THE NASA ICING RESEARCH TUNNEL UNDER SEVERE ICING AND DRY-AIR CONDITIONS

W. Olsen, J. Van Fossen, and R. Nussle
National Aeronautics and Space Administration
Lewis Research Center
Cleveland, Ohio 44135

SUMMARY

Measurements were made of the pressure drop and thermal performance of the unique refrigeration heat exchanger in the NASA Lewis Icing Research Tunnel (IRT) under severe icing and frosting conditions and also with dry air. This information will be useful to those planning to use or extend the capability of the IRT and other icing facilities (e.g., the Altitude Wind Tunnel (AWT)).

The IRT heat exchanger and refrigeration system is able to cool the air passing through the test section down to at least a total temperature of -30 °C (well below the requirements of icing), and usually up to -2 °C. The system maintains a uniform temperature across the test section at all airspeeds. Holding a uniform temperature is more difficult and time consuming at low airspeeds, at high temperatures, and on hot humid days when the cooling towers are less efficient.

Tests show that the very small surfaces of the heat exchanger prevent any icing cloud droplets from passing through it and going through the test section again. The original designers of the IRT recognized that the heat exchanger would be the major pressure drop component; accordingly, they designed the heat exchanger so that it would not be adversely affected by severe icing.

The effect of severe icing on the pressure drop and thermal performance of the heat exchanger was measured. Worst-case icing nearly tripled the pressure drop, and an increase in the fan speed (rpm) was required to maintain a constant airspeed in the test section. During this test the heat exchanger iced up uniformly enough that the temperature uniformity was no worse than about ±1 °C.

The overall conclusion is that the IRT heat exchanger, which was designed and built more than 40 years ago, is a sophisticated unique design that performs superbly and is necessary for icing research.

It has been suggested that an IRT heat exchanger design of increased face area be used for the proposed AWT, and that it be located in the same place as the old AWT heat exchanger. Measurements of the IRT heat exchanger performance showed that it would meet the dry-air pressure drop and heat transfer goals as well as the proposed AWT heat exchanger. It should also perform better under severe icing and frosting conditions.

E-3661

INTRODUCTION

A schematic of the NASA Icing Research Tunnel (IRT) is shown in figure 1. The refrigeration heat exchanger is located upstream of the test section and downstream of the tunnel fan. The refrigeration heat exchanger in the IRT has three primary tasks: (1) to cool the airflow to the temperatures required for icing tests and for a minimum pressure drop; (2) to maintain a uniform temperature and velocity across the test section even after long severe icing sprays; and (3) to completely remove the droplets of the icing spray cloud.

Old documents in the historical file of the IRT (c. 1943) indicate that the original designers of the IRT recognized the following in their selection of the IRT refrigeration heat exchanger configuration. The heat exchanger has the largest pressure drop of any component in the closed tunnel loop. As the icing-cloud droplets accrete on the very small surfaces of the heat exchanger, the air passages become partially blocked, and the pressure drop across the heat exchanger increases. If the heat exchanger surfaces accrete ice nonuniformly, the airspeed and air temperature across the test section could become unacceptably nonuniform.

The main purpose of this paper is to document the IRT heat exchanger performance data. These data include the overall thermal performance and pressure drop in dry air and also after severe icing lasting a long time. The practical operating limits of the refrigeration system are discussed. This information will be useful to the users of the IRT and other icing facilities, and to people who plan to expand the capabilities of icing simulation facilities such as the IRT.

APPARATUS AND PROCEDURE

The following are described in this section: the NASA Icing Research Tunnel (IRT), the refrigeration heat exchanger, and the refrigeration system. The instrumentation and test procedure used to determine the performance of the heat exchanger are also described.

Icing Research Tunnel

The IRT is a closed-loop refrigerated wind tunnel with a test section that is 1.8 m high by 2.7 m wide (6 ft high by 9 ft wide). The airspeed in the test section can be varied from 40 to 480 km/hr (25 to 300 mph). The total air temperature can be independently varied from about -2 to -30 °C (28 to -22 °F). (The IRT has been operated at -40 °C, but icing requires only -30 °C.) Spray nozzles are used to produce the icing spray cloud with a liquid water content (LWC) that can be varied from about 0.2 to 3.0 g/m^3 and drop sizes that can be varied independently from a median volume drop size (MVD) of about 5 to 40 μm. Because of spray pressure limits, not all combinations of LWC and drop size can be attained at all airspeeds. For a discussion of the spray cloud calibration and possible error sources, refer to the appendix in reference 1.

Refrigeration Heat Exchanger

The refrigeration heat exchanger is located downstream of the tunnel drive fan and upstream of the spray nozzles. The spray nozzles are upstream of the test section (fig. 1). There are unheated turning vanes upstream and downstream of the heat exchanger.

The refrigeration heat exchanger has eight identical heat exchanger units, each spanning the 8.8-m (29-ft) wide IRT duct (Blueprints of heat exchanger, IRT historical file c. 1943.) Figure 2 is a sideview of these eight units, which make up the folded heat exchanger shape in the IRT. The heat exchanger was folded to fit in the IRT and to have enough area to cool the airflow sufficiently. Sheet-metal turning vanes on the downstream face of the heat exchanger were Carrier's solution to straightening the airflow and keeping the pressure drop low. Each heat exchanger unit is eight tubes deep. The tubes are in line, with a tube spacing (pitch) of 3.8 cm (1.5 in.), center to center, in a square array as shown by the detail sketch in figure 3. The fins are continuous thin sheets of galvanized steel. The fin spacing is wide to reduce the effects of icing and frost (3 fins/in). As will be seen, the cloud is totally caught by the heat exchanger surfaces because of their small dimensions and also because of the severe turn the airflow must make when going through it. The important dimensions for the IRT heat exchanger are listed on tables I and II.

Care was taken by the designers at Carrier Corporation in 1943 (Carrier Instruction Manual for Refrigeration Plant at NACA, Cleveland, OH, Government Contract No. NAW-1460; 1944. IRT historical file.) to ensure that the air temperature and airspeed downstream of the heat exchanger would be uniform. To maintain uniform heat exchanger wall temperatures, the pressure in the heat exchanger tubes is kept constant by four means (fig. 3): (1) To compensate for the pressure-head differences during operation (at constant flow) an orifice plate in each of the five supply lines was drilled by trial and error after the heat exchanger was installed. (2) Only a small fraction of the refrigerant (Freon 12) in the heat exchanger tubes boils to ensure that there will be very little pressure drop. (3) These tubes are supplied by and exhausted into large manifolds. (4) The combined two-pass parallel and countercurrent heat exchanger arrangement is also important in keeping the temperatures uniform. The pressure drop across the orifice plate at the entrance also assures stable boiling in the tubes. The above measures, the fairly uniform airflow, and the droplet mixing in the airstream all help ensure that frosting and icing are uniform and have a minimum effect during long severe icing tests.

Simplified Description of Refrigeration System

The essentials of the refrigeration system (Carrier Instruction Manual for Refrigeration Plant at NACA, 1944) are shown schematically in figure 4. It consists of two fluid flow loops that mix together in the flash cooler where the liquid and vapor are separated by gravity and screens. The following is a simplified description of how each fluid loop of the refrigeration system works.

Liquid Freon 12 is pumped from the bottom of the flash cooler (separator) in the refrigeration building to the IRT. Outside the IRT, the flow is divided

into five lines which supply the eight heat exchanger units. Units 2 and 3, 4 and 5, and 6 and 7 share three lines as shown in figures 2 and 4, while units 1 and 8 have their own supply lines. Orifices in the five liquid supply lines compensate for the pressure-head differences. Less than half of the liquid Freon is boiled in the heat exchanger tubes to cool the tunnel airstream. As a consequence there is very little pressure drop in these tubes and, therefore, the heat exchanger wall temperatures tend to stay uniform. The two-phase liquid-vapor fluid flows back to the flash cooler in the refrigeration building where the vapor is separated from the liquid. This liquid is mixed with the cold liquid from the compressor-cooler loop, and the cooled liquid is pumped back to the IRT heat exchanger.

The compressor-cooler loop pulls out the vapor from the flash cooler through damper valves, which are used to control the pressure in the flash cooler (which should be called the separator). Since the liquid in the flash cooler is saturated, the pressure in the flash cooler regulates the temperature. The pressure drop in the large return line is small so that the wall temperature of the heat exchanger will be close to the saturation temperature in the flash cooler. By adjusting the damper valve, the saturation temperature of the Freon can be changed to obtain the desired air temperature in the IRT. The refrigeration operators try to keep the saturation temperature about 5 °C (10 °F) below the desired air temperature. They slowly increase this temperature difference as the heat exchanger accumulates ice and frost. At the higher air temperatures steam heating of the first two turning vanes is turned on to increase the refrigeration load and permit more accurate control. After the Freon vapor passes through the damper valve, it passes to a header which is connected to 13 compressor-condensor-economizer loops. The vapor in each loop passes through a four-stage compressor and then to the condensor where the vapor becomes a hot liquid. Heat is rejected from the compressor-cooler loop by the condensor, which is cooled by water from the cooling tower. The hot liquid flows to the economizer where it is flash cooled through two stages of pressure drop and converted into cold liquid. The flashed vapor is piped back to the second and third stages of the compressor. The cold liquid from each compressor loop flows into the separator where it mixes with the hotter liquid coming back from the heat exchanger that cools the IRT airstream.

The refrigeration plant (fig. 5) was originally designed to cool the very large Altitude Wind Tunnel; it is still the largest direct expansion plant in the world. The IRT has used 3 to 10 of the 13 compressors.

Two additional systems should also be mentioned briefly. One system permits the heat exchanger to be defrosted with warm liquid Freon from the separator. The warm liquid is obtained by reducing the flash cooling in the economizer. Experience has shown that defrosting is not necessary because the IRT heat exchanger is insensitive to even severe icing and frosting. However, the defrosting system is still used on a few compressor loops for fine-tuning heat addition. The other system is a steam heat exchanger which was used to heat the tunnel airstream to higher uniform air temperatures than can be presently maintained. This heat exchanger was removed many years ago because of steam leaks. Higher uniform air temperatures in the IRT are necessary for icing research near and above incipient freezing. Higher air temperatures could also be obtained by other methods which are discussed later in this paper.

Test Instrumentation

Only a limited amount of very simple instrumentation was added to the standard IRT instrumentation in order to measure additional critical data. The pressure drop across the heat exchanger, Δp_H, was measured with two total-pressure probes located upstream and downstream of the heat exchanger, as shown in figure 1. The pressure drop was measured with an inclined manometer which can measure a difference of 0.025 cm (0.01 in).

Velocity surveys were measured upstream and downstream of the heat exchanger (Cubbison, R.W.; Newton, J.R.; and Schabes, H.: Total Pressure Loss Across the Icing Research Tunnel Cooler for Test Section Indicated Airspeeds of 75 to 250 mph. Internal Report, Icing Research Tunnel, NASA Lewis Research Center, Cleveland, Ohio). Figure 6 shows that the velocity downstream of the heat exchanger varies no more than ±10 percent over most of the duct. These surveys show that the heat exchanger successfully performed its task of making the velocity more uniform than that produced by the fan. These velocity profiles also show that the single-point pressure probes give an accurate measure of the pressure drop because the velocity head is such a small contribution to the total pressure at these low airspeeds. The downstream velocity profiles suggest that the turning vanes on the downstream face of the heat exchanger turned the airflow a bit too much. In any event, the contraction ratio of the IRT is so large (14:1) that a uniform velocity across the test section would probably have occurred even if there was no heat exchanger in the IRT to help make the flow uniform. The large contraction ratio would also mitigate the consequence of nonuniform icing of the heat exchanger.

Thermocouples on the IRT turning vanes upstream and downstream of the heat exchanger were used to measure the air temperatures. These thermocouples have droplet shields so that they sense only the temperature of the dry air. Ten thermocouples are distributed over the entire downstream turning vane array. These thermocouples are used to determine the spatial uniformity of the total air temperature across the heat exchanger and also across the test section. The spatial uniformity was almost always uniform to ±1/2 °C (±1 °F); therefore, only the center thermocouple readings will be reported. There are only two thermocouples on the upstream turning vanes, straddling the center. All thermocouples were checked by immersion in an ice bath; they were all within 1/2 °C (1 °F) of the freezing point.

A few thermocouples were attached to the copper tubes of the heat exchanger for all but the first few tests. These tube temperatures were always about 2 °C warmer than the saturation temperature in the flash cooler (separator). This temperature difference is caused mainly by the pressure drop in the refrigerant return line. Therefore, wherever tube temperature data was not obtained, 2 °C was added to the saturation temperature of the separator. The tube temperature is needed to calculate the log mean temperature difference (LMTD). All other reported data used existing IRT instrumentation (e.g., the fan speed (rpm) and power).

Test Procedure

The heat exchanger performance tests involved tests with dry air and with icing. For the dry air tests (i.e., no spray), the tunnel was brought to the

desired airspeed and air temperature. The total temperature in the test section is the static air temperature measured at the IRT turning vanes upstream of the spray system. The pressure drop, temperatures, and other data were recorded when the readings were steady. The procedure for the icing tests of the heat exchanger was the same as for the dry air tests except that the total pressure probes upstream and downstream of the heat exchanger were capped before each icing spray to prevent icing cloud droplets from plugging the tubes. After the icing run, the caps were removed, and the tunnel was returned to the desired airspeed to measure the pressure drop. The tubes were then capped, and another part of the total icing-spray time was added. The ice accretion on the heat exchanger surfaces was measured at the end of the total icing-spray time. Ice accretion on all parts of the IRT tunnel loop was measured at the end of some of these heat exchanger tests (ref. 2).

The steam heat to the turning vanes was off during all these heat exchanger tests. However, the other important heat sources remained: the fan pumping work (the fan motor is cooled separately), steam heat to the spray bars, and heat from the outside coming through the insulated walls of the tunnel loop. When spraying, there is also heat from the heated spray air and water.

RESULTS AND DISCUSSION

The experimental results for this paper are reported in four parts. The dry-air results, which include pressure drop and thermal performance data, are discussed first. The data showing the effect of severe icing on the pressure drop and thermal performance are discussed next. The third part is a short simplified discussion of the operating limits of the refrigeration system based on operational experience. The last part involved scaling up these results to a larger IRT heat exchanger that could have been installed in the proposed altitude wind tunnel.

Dry-Air Results

Pressure drop across heat exchanger. - The IRT was run over a range of airspeeds, and the pressure drop across the heat exchanger Δp_H was measured for several air temperatures. No spray was used, and visual inspection showed that there was no frost from water vapor on the heat exchanger surfaces. Table III contains the measured data. The dimensionless loss coefficient K was calculated according to standard practice from equation (1) and the results are listed in table III.

$$K = \frac{\Delta p_H}{1/2 \rho_H V_H^2} \tag{1}$$

(Symbols are defined in the appendix.) The average velocity through the duct containing the heat exchanger V_H was calculated from the airspeed in the test section and the areas of those ducts.

$$V_H = \frac{A_T}{A_H} V_T = \frac{V_T}{14} \tag{2}$$

The average loss coefficient K was 3.88, with no discernible effect of airspeed and air temperature on K. This value of K includes all duct to heat exchanger losses, including the losses resulting from the bent fins and corrosion of the 40-year-old heat exchanger. Later in this report we will scale this result to the higher air mass flow for the AWT heat exchanger.

Heat transfer. - Eleven dry-air conditions were run to measure the thermal performance of the heat exchanger in dry air. The airspeeds and temperatures run are listed in table III along with the thermal performance data for the IRT heat exchanger. The terms in table III are either measured directly or calculated from the equations presented here.

The temperature reduction across the heat exchanger is equal to air temperature upstream minus the air temperature downstream:

$$\Delta T = T_{up} - T_{down} \tag{3}$$

As previously explained, only the temperatures along the centerline of the tunnel are used because the air temperatures measured across the heat exchanger duct were uniform to about $\pm 1/2$ °C (± 1 °F).

The mass flow through the heat exchanger is calculated from the mass flow through the test section:

$$\dot{m} = \rho_T A_T V_T = \rho_H A_H V_H \tag{4}$$

The density of the air is calculated with the ideal gas equation from the pressure and temperature at that location.

The heat removed from the air is calculated from

$$Q = \dot{m} c_p \Delta T \tag{5}$$

The log mean temperature difference, which is the characteristic temperature difference used for heat exchangers, is given by the following equation:

$$LMTD = \frac{(T_{up} - T_{w,up}) - (T_{down} - T_{w,down})}{\ln\left(\frac{T_{up} - T_{w,up}}{T_{down} - T_{w,down}}\right)} \tag{6}$$

The wall temperature of the heat exchanger tubes T_w was measured by thermocouples that were attached to the copper tubes. These thermocouples were not attached to the tubes for the early test runs. But it was found that the tube wall temperatures were uniform, and the difference between the refrigerant temperature in the flash cooler (separator) T_F and the tube wall temperatures T_w was always nearly 2 °C. Therefore, the LMTD was calculated for all test runs by using the following approximate equation:

$$LMTD = \frac{T_{up} - T_{down}}{\ln\left(\frac{T_{up} - T_w}{T_{down} - T_w}\right)} \tag{7a}$$

where the wall temperature is

$$T_W = T_F + 2 \tag{7b}$$

The overall heat transfer coefficient U can be calculated from the following equation:

$$Q = UA(LMTD) \tag{8}$$

We only calculated the multiple of U and the area UA because no further detail is required for this study. Figure 7 contains the UA data plotted against the Reynolds number. The Reynolds number is based on the hydraulic diameter of the IRT heat exchanger air passages d_h and the area of the duct in which the heat exchanger is installed.

$$Re = \frac{\dot{m} d_h}{A_H \mu} \tag{9}$$

The UA data generally follow a 0.8 power law with Reynolds number. Figure 7 will be used later to scale up to the AWT application.

Results for Worst-Case Icing and Frosting Conditions

The effect on the heat exchanger performance of several different worst-case icing and frosting conditions is discussed in this section. Figure 8 is a photograph of part of the heat exchanger with a good coating of ice. Icing increases the flow resistance (i.e., pressure drop) and the thermal resistance of the heat exchanger. The heat exchanger is the dominant flow resistance in the IRT tunnel loop. These detrimental changes must be compensated for by increasing the fan speed (rpm) and refrigeration power consumption. Therefore, it is quite possible that a large ice buildup on the heat exchanger surfaces could cause the fan or refrigeration system to reach some limit while attempting to maintain a constant airspeed and temperature in the test section. The changes caused by severe icing and the system limits are discussed in this section. But first, the severe ice and frost accumulations used in these studies are described along with the icing cloud stopping ability of the heat exchanger.

Description of worst-case ice and frost accumulations. - We must start with a definition of worst-case icing and frosting conditions. The heat exchanger has several tasks in an icing wind tunnel. As will be seen later, it must deliver cold air that is controlled and uniform to better than ±1 °C (±2 °F), preferably ±1/2 °C. The heat exchanger must ice up uniformly so that the airflow will remain uniform across the test section. It must remove all of the icing cloud to eliminate the possibility that partially frozen droplets will go around the tunnel loop and reenter the test section. The worst-case conditions are clearly those where the heat exchanger cannot perform all of the above tasks. A number of icing conditions were selected, based upon previous experience, that were thought to be capable of causing the heat exchanger to fail in performing some of the above tasks. These selected conditions are listed in table IV.

The ice and frost accumulations on the heat exchanger for the runs in table IV are sketched in figure 9. The accumulations shown were measured at the end of these runs. Before and after photographs of the ice accumulation for run 5/11 are shown in figure 10.

The two runs that stand out as having the worst flow blockage are runs 7/11 and 8/2 (figs. 9(b) and (c), respectively). The worst blockage occurred at -29 °C (-20 °F). But the cause of this worst-case accumulation was the frost that occurred from the supersaturated vapor, thought to be caused by an abnormal leakage of hot humid air from the outside. Run 5/11 (fig. 9(a)) had even smaller droplets and was just as cold; however, that run did not have as much frost blockage because the vapor was not supersaturated. Figure 10 shows a small portion of the upstream face of the heat exchanger before and after the icing of run 5/11. The least blockage occurred with the large-drop-size sprays (e.g., figs. 9(d) and (e)). In all cases the ice accretion was white rime ice mixed with a little bit of frost from the vapor. Nearly all accumulation is on the leading edge of the fin sheet and the leading edges of the first few tubes. The last four tubes of the eight in line, accumulated no ice from the cloud droplets and little frost from the vapor. The turning vanes on the downstream face of the heat exchanger (figs. 2 and 3) also accumulated only a few small patches of frost.

At this point the discussion is temporarily changed to the heat exchanger task of removing all of the icing cloud. To determine if any cloud droplets passed through the heat exchanger, a very fine screen was located downstream of the heat exchanger and upstream of the spray bars. The wires were so thin and closely spaced they would catch any droplets that made it through the heat exchanger. None of the worst-case icing sprays listed in table IV, except one exceptional run discussed below, caused any ice (from the spray droplets) or frost (from the vapor) to collect on the screen. In other words, the heat exchanger stopped the spray droplets completely. Supporting this conclusion were laser spectrometer measurements (personal communication with R. Ide) which revealed that only very small droplets (less than 5 μm) pass through the heat exchanger and only when the temperature is above about -2 °C (28 °F). Detailed ice accretion mass balances on the IRT were made (ref. 2) while the heat exchanger measurements were being made. These mass balances show the fraction of the total cloud-droplet mass that the heat exchanger and the other components of the IRT tunnel loop caught. The heat exchanger removes 90 percent of the 10-μm (volume median) cloud, 75 percent of the 20-μm cloud, and 65 percent of the 30-μm cloud. The two turning vane sets upstream of the fan and the fan blades remove most of the big droplets of the spray distribution, which means that the small surfaces of the heat exchanger have to remove the remaining small droplets of the spray distribution. These remaining droplets are so small that the turning vane upstream of the heat exchanger never shows any ice accretion (i.e., catches no droplets).

In the one exceptional run just discussed, a coating of frost formed on the fine screen located downstream of the heat exchanger (run 8/2 in table IV). There was so much frost from the vapor that there was loose frost on the floor downstream of the heat exchanger. However, that run was abnormal because the air was supersaturated with water vapor (as evidenced by a visible cloud in the test section). This excess vapor was caused by abnormal air leakage into

the tunnel of the hot, humid air outside that day. This run caused the formation of the greatest amount of frost on the heat exchanger surfaces, which adversely combined with ice from the cloud droplets (fig. 9(c)). The airflow through the heat exchanger was nearly blocked in less than 30 min. (The leakage of outside air through bad tunnel-access door seals must be stopped, mainly because pressure tubes of an unheated pitot tube plug up quickly when there is a visible cloud in the test section.) It is interesting that except when there is outdoor air leakage into this closed-loop tunnel, the IRT is not normally troubled by frosting from the vapor, in spite of the icing cloud spray from which some vapor is continually generated by the evaporation of the droplets.

Dew point measurements downstream of the heat exchanger and upstream of the droplet spray bars show that the relative humidity there stays approximately constant at 70 percent no matter what the airspeed or temperature, especially after the first icing spray run. Calculations show that very little droplet mass is evaporated and that the relative humidity in the test section is essentially 100 percent (ref. 1). The absence of a frosting blockage problem in the IRT is probably largely due to the fact that cold air can hold very little vapor mass compared to warm air. Another reason is that the designers of the IRT heat exchanger selected a wide fin spacing (3 fins/in.) to prevent the heat exchanger from becoming blocked with frost. They based their heat exchanger selection upon experience with refrigeration heat exchangers in meat-packing plants, which are always subjected to warm humid air (documents in IRT historical file, c. 1943 to 1945).

Pressure drop. - The pressure drop across the heat exchanger will increase as ice and/or frost accumulate on the heat exchanger surfaces. The accumulation is mainly on the leading edges of the fin sheet and the first few refrigerant tubes. Figure 11 shows how the flow loss coefficient K (defined by eq. (1)) increases with corrected time for the severe icing conditions just described. In these tests, the fan speed (rpm) was increased as ice accumulated to maintain the same air mass flow through the heat exchanger. Corrected times τ_c are used so that each icing run with different icing conditions is compared at the same incoming droplet mass (i.e., $(LWC)(V)(\tau)$ = constant).

$$\tau_c = \frac{(LWC)VX}{(LWC)_{ref}V_{ref}X_{ref}} \cdot \tau \qquad (10)$$

where the reference conditions are $(LWC)_{ref}$ = 1.36 g/m^3, V_{ref} = 240 km/hr (150 mph), and X_{ref} = 0.85. The term X is the fraction of cloud mass that reaches the heat exchanger because it was not caught by the tunnel components upstream (ref. 2).

Notice that all of the data in figure 11 share the same change in K per unit corrected time (i.e., same slope), except for one point. The pressure drop increased dramatically after the 24-min (corrected time) data point of run 8/2 because the heat exchanger became nearly plugged with ice and frost (as depicted in fig. 9(c)). As said previously, this run was not typical because the rapid plugging was mainly caused by frost from the large amount of vapor that leaked into the tunnel. Nevertheless, all icing runs will eventually cause the heat exchanger to plug up, and the pressure drop will then rise dramatically. Experience has shown that even a long evening of severe icing will not cause the IRT heat exchanger to come close to plugging up.

Before the heat exchanger is close to plugging up, the temperatures downstream of the heat exchanger become unacceptably nonuniform across the duct (i.e., more than ±1 °C (±2 °F)). This excessive nonuniformity occurred only for that nearly plugged data point of run 8/2.

Heat transfer. - The effect of icing and frost accumulation on the heat exchanger thermal performance is shown in figures 12 and 13. These figures contain a plot of the data for one icing run (run 5/11). This run is fairly typical of the results for the other worst-case icing conditions (table IV). Figure 12 shows that the fan speed (rpm) and power consumption were increased in order to maintain a constant airspeed in the test section (i.e., constant air mass flow). The fan blades and turning vanes of the IRT accumulate ice, which reduces their aeroperformance and requires a greater fan speed (rpm) and power consumption. This, in turn, required an increase in the amount of heat removed by the heat exchanger. To maintain a constant air temperature downstream of the heat exchanger, the heat removal was increased by lowering the Freon coolant temperature in the heat exchanger tubes (fig. 13). The icing and frosting decreased the thermal conductance of the heat exchanger UA which required an even greater reduction in the Freon temperature T_F to compensate. The refrigeration operators manually maintain the required downstream air temperature (i.e., test section total air temperature) by adjusting the refrigerant temperature (i.e., the pressure in the flash cooler). At the higher air temperatures and at low airspeeds, they find it helpful to add steam heat to the turning vanes (fig. 1) in order to provide a minimal load for the refrigeration plant.

Operating Limits of the IRT Refrigeration System and Proposed Improvements

The operating limits of the IRT refrigeration system are characterized by the maximum and minimum air temperatures that can be attained and held uniform across the test section. In most instances the air temperatures stay uniform within ±1/2 °C (±1 °F) up to a total temperature of -2 °C (28 °F) and down to -30 °C (-22 °F) for airspeeds above approximately 130 km/hr (80 mph). The IRT was once tested down to -45 °C; however, temperatures below -25 °C (-15 °F) are rarely required for icing tests. An experienced operator on the manually controlled refrigeration system can usually attain in a reasonable time a uniform temperature for total temperatures up to -2 °C (28 °F) or for airspeeds down to 40 km/hr (25 mph, the fan idle speed). Such performance is impossible on hot humid days because the heat rejection from the cooling towers is greatly diminished.

The heat exchanger configuration was selected by the IRT designers because the pressure drop would increase only slowly in severe icing and frosting conditions. Furthermore, every effort was made to ensure that the heat exchanger iced up uniformly so that the airflow and air temperature would remain uniform. The heat exchanger designers at Carrier Corporation (c. 1943) were very successful; the usual nonuniformity of ±1/2 °C (±1 °F) increased to no worse than ±1 °C (±2 °F) after a long period of severe icing.

One obvious question is, How closely and uniformly does the air temperature have to be controlled and repeatable in order to do quality research in an icing tunnel? Ice shapes and their resulting drag penalty are the most sensitive to any error in air temperature. Figure 14 contains data measured

in the IRT which shows how the ice shape and resulting drag coefficient change when only the air temperature is changed. The ice shape and drag coefficient change very little when rime or near-rime ice are formed. When glaze ice is formed the drag coefficient changes rapidly with temperature; here is where close temperature control may be needed. For comparison, the ±1/2 °C and ±1 °C error and nonuniformity bands are indicated in the figure. The close temperature control and uniformity that the IRT can achieve appear to be necessary with glaze ice, but not for rime ice.

There is no external control of temperature uniformity. Nevertheless, experienced refrigeration system operators can rapidly achieve a new air temperature that is uniform; inexperienced operators often require a long time to attain uniformity. How can the operator have such an effect on temperature uniformity when he can only control the pressure in the flash cooler? The writers believe the reason may be short-term nonuniform boiling and flow in the eight heat exchanger units which can persist for a long time. This time transient can be greatly reduced if the operator instinctively follows some ideal pressure-time schedule for the conditions (e.g., the desired air temperature, the cooling load, the icing and frosting conditions of the heat exchanger, and the outside air temperature and humidity). An automatic refrigeration controller using an artificial intelligence program would probably be helpful when inexperienced refrigeration plant operators are used.

A number of improvements have been incorporated into the refrigeration system and operating procedures in the last few years. One of these improvements is the installation of a modern computer-controlled automatic control system with a manual override. It is expected that this new system will result in more rapid temperature control while maintaining uniform temperatures. Increased air temperatures are necessary so that incipient-freezing icing conditions can be investigated. To accomplish this task, future improvements have been proposed that involve rebuilding the refrigeration compressors so that they can reach higher suction and discharge pressures and using the defrosting system to effectively bypass the cooling by the economizer. Raising the ΔT by a steam heat exchanger, or exchanging outside air would be another way. The proposed future high-speed insert for the IRT will require even higher air temperatures to attain incipient freezing. The insert will require additional improvements to the refrigeration system, such as a different refrigerant fluid.

An IRT Type of Heat Exchanger Used in the Proposed Altitude Wind Tunnel

In this section the number of IRT heat exchanger units will be increased analytically to fill the much larger duct of the AWT. The heat exchanger fold geometry would be exactly the same as the old AWT heat exchanger. In other words, the configuration sketched in figure 2 will be the same except that there will be many more zigzag folds than in the IRT. The question being asked is, Will this larger heat exchanger face area meet the AWT requirements for pressure drop and heat transfer for dry air and for severe icing conditions? These scaled-up results will be compared with equivalent experimental results for the nominal AWT heat exchanger that were reported by Cubbison, Newton and Schabes. (Total Pressure Loss Across the Icing Research Tunnel Cooler for Test Section Airspeeds of 75 to 250 mph. Internal Report, Icing Research Tunnel, NASA Lewis Research Center, Cleveland, Ohio.)

Pressure Drop for Dry Air. - The maximum pressure drop for the AWT with dry air can be calculated by using the flow loss coefficient K that was measured for the IRT heat exchanger. Measured K was found to be independent of flow; average K was found to be 3.83. The maximum pressure drop that would occur at the maximum air mass flow expected for the AWT, can be calculated from equation (1), which is written here again as

$$\Delta p_H = K \frac{\rho_H V_H^2}{2_g} = \frac{K}{2_g \rho_H} \frac{\dot{m}^2}{A_H} \tag{11}$$

For the maximum mass flow in the AWT, $\dot{m}$ = 4990 kg/sec (11 000 lb/sec), the velocity through the 15.2-m (50-ft) diameter heat exchanger duct upstream of the test section would be 88 km/hr (55 mph). The velocity through each section of the folded IRT heat exchanger would be only 24 km/hr (15 mph). The pressure drop across this AWT heat exchanger at the maximum air mass flow would be 14.5 cm (5.7 in) of water. This pressure drop is below the goal of 15 cm (6 in) of water.

Thermal performance for dry air. - The overall heat transfer per deg C, UA was measured for the IRT heat exchanger and plotted in figure 7 against Reynolds number. The maximum UA needed for the AWT is 1400 kW/°C (2.7×10^6 Btu/hr °F), which occurs at an air mass flow of 2490 kg/sec (5484 lb/sec). The Reynolds number for the maximum duct airspeed for the IRT heat exchanger configuration installed in the 15.2-m (50-ft) diameter duct of the AWT is 9800. At that maximum Reynolds number the maximum UA for the size of the IRT heat exchanger would be 660 kW/°C (1.25×10^6 Btu/hr °F). But the 15.2-m (50-ft) diameter duct where the heat exchanger would be installed is 2.7 times larger than the duct of the IRT heat exchanger. Therefore, the UA for the IRT heat exchanger enlarged to fit in the AWT would be 20 percent larger than the maximum UA required.

These values of pressure drop and UA for the IRT heat exchanger sections fitted into the AWT are now compared with the values for the nominal AWT heat exchanger that were measured in reference 3. That nominal heat exchanger was fitted into a larger duct (i.e., a blister) to increase the overall face area of that straight through heat exchanger. The measured dry-air pressure drop was exactly the same as the pressure drop for the IRT heat exchanger when both were scaled to the maximum mass flow. Actually, the nominal heat exchanger has a somewhat larger pressure drop when you include the pressure drop caused by the area change of the blister. The maximum dry air UA was also exactly the same as the IRT heat exchanger after appropriate scaling. On the negative side, the IRT heat exchanger may cost more to fabricate than the nominal AWT heat exchanger configuration.

Effect of icing and frosting. - An attempt was made to analytically compare the icing results observed herein for the full IRT heat exchanger with the icing results reported in reference 3 for a small sample of the nominal AWT heat exchanger. Unfortunately this could not be accomplished with sufficient accuracy because the experimental conditions were not sufficiently comparable. It turns out that a quantitative comparison is not required anyway. Reference 3 noted that the AWT heat exchanger plugged up very quickly from frost (from the vapor) and icing (from the cloud droplets). In contrast, the IRT heat exchanger kept on cooling and maintaining a uniform temperature under

extremely severe icing and frosting conditions. These observations reinforce the fact that the AWT heat exchanger should have followed the standard design requirement for heat exchangers subject to severe frosting (e.g., food storage applications)- use a wide fin spacing (3 or 4 fins per inch). The nominal AWT heat exchanger was to be built with eight fins per inch while the IRT heat exchanger uses four fins per inch.

CONCLUDING REMARKS

Measurements were made of the pressure drop and thermal performance of the refrigeration heat exchanger in the NASA Icing Research Tunnel (IRT) under severe icing and frosting conditions and also with dry air.

The IRT heat exchanger and refrigeration system is able to cool the air passing through the test section down to at least a total air temperature of -30 °C (well below the requirements of icing) and usually up to -2 °C. It inherently maintains a uniform temperature across the test section within about ±1/2 °C at all airspeeds. Obtaining a uniform temperature is more difficult and time consuming at higher air temperatures (near 0 °C), at low airspeeds, and when the cooling towers are less effective on hot and humid days.

Extensive additional measurements indicate that the very small surfaces on the heat exchanger prevent the icing cloud from passing through and reentering the test section. The original designers of the IRT recognized that the heat exchanger would be the major pressure drop component; accordingly, they designed a heat exchanger configuration that should not be adversely affected by severe icing.

The effect of severe icing on the pressure drop and thermal performance of the heat exchanger was measured. The worst-case icing nearly tripled the pressure drop, requiring the fan speed to be increased to maintain a constant airspeed in the test section. During this test the heat exchanger iced up uniformly enough that the temperature uniformity was no worse than about ±1 °C.

The overall conclusion is that the heat exchanger that cools the IRT, which was built more than 40 years ago, is a sophisticated design with superb performance. The close temperature control and uniformity of the IRT appears to be necessary for ice accretion research.

APPENDIX - SYMBOLS

A_H	cross sectional area of duct where heat exchanger is installed, m^2
A_T	cross sectional area of the test section, m^2
c_p	specific heat of air, W-sec/kg-°C
d_h	hydraulic diameter of heat exchanger air passages between tubes, m
K	flow coefficient defined by eq. (1), ND
LMTD	log mean temperature difference defined by eq. (6), °C
LWC	liquid water content, g/m^3
MVD	median volume drop size, μm
m	air mass flow through the heat exchanger, kg/sec
P_v	pressure (saturation) in the flash cooler, N/m^2
Δp_H	pressure drop across the heat exchanger, N/m^2 or cm of H_2O
Q	heat removed from the air by the heat exchanger, eq. (5), W
Re	Reynolds number based on the hydraulic diameter, eq. (9)
T_{down}	average air temperature downstream of the heat exchanger, °C
T_F	temperature of the saturated Freon in the flash cooler, °C
T_{up}	average air temperature upstream of the heat exchanger, °C
T_w	wall temperatures of Freon tubes that make up heat exchanger, °C
ΔT	temperature drop across the heat exchanger, eq. (3), °C
UA	overall heat transfer per unit temperature of air cooled; W/°C
V_H	airspeed through the heat exchanger duct, m/sec
V_T	airspeed in the test section, m/sec
X	fraction of the cloud mass sprayed that reaches the heat exchanger
τ_c	corrected time; eq. (10), min
μ	dynamic viscosity of air, kg/sec-m
ρ	air density, km/m^3

REFERENCES

1. Olsen, W.; Tacheuchi, D.; and Adams, K.: Experimental Comparison of Icing Cloud Instruments in the NASA Icing Research Tunnel. AIAA Paper 83-0026, Jan. 1983. (NASA TM-83340).

2. Newton, J.E.; and Olsen, W.: Study of Ice Accretion on Icing Wind Tunnel Components. AIAA Paper 86-0290, Jan. 1986. (NASA TM-87095).

3. Van Fossen, G. J.: Heat Transfer and Pressure Drop Performance of a Finned-Tube Heat Exchanger Proposed for Use in the NASA Lewis Altitude Wind Tunnel. NASA TM-87151, 1985.

TABLE I. - TUBES AND FINS OF ICING RESEARCH TUNNEL (IRT) AND PROPOSED NOMINAL ALTITUDE WIND TUNNEL (AWT) HEAT EXCHANGERS

	IRT heat exchanger	Nominal AWT heat exchanger
Tubes:		
Arrangement	8 tubes, in line (square pitch, 3.8 cm)	6 tubes, staggered (equilateral triangle, 6.4cm)
Material	Copper	Copper
Diameter, cm	0.95	2.5
Wall thickness, cm	.12	0.21
Fins:		
Arrangement	Continuous sheet	Circular (1.6 cm high)
Material	Galvanized steel	Copper
Thickness, cm (in.)	0.078 (0.032)	0.041 (0.016)
Number per inch	3	8

TABLE II. - OVERALL DIMENSIONS OF HEAT EXCHANGERS

Descriptions	IRT folded heat exchanger	IRT-type heat exchanger for use in AWT	Nominal AWT heat exchanger
Configuration and location	Folded W	Same as IRT, but more folds and sections	Cross flow in blister before corner 3
Duct area, m^2	72.8	190	[a]365
Face area, m^2	259	[a]652	[a]340
Minimum flow area, m^2	176	[a]443	[a]182
Active tube length, m	53 900	[a]136 500	[a]24 800

[a]Assumes 93 percent of duct area is filled with heat exchanger sections, which is the same as the old AWT heat exchanger.

TABLE III. - DRY-AIR PERFORMANCE DATA FOR IRT HEAT EXCHANGER

Run	Airspeed, V_T, km/hr	Air temperature, °C		Freon temperature, T_F, °C	Pressure drop, ΔP_H, cm H_2O	Loss coefficient, K	Reynolds number, Re	Heat removed, Q, kW	Overall heat transfer per unit temperature of air cooled, UA, kW/°C	Log mean temperature difference LMTD, °C	Mass flow, m, kg/sec
		T_{down}	T_{up}								
5/10	241	-12	-10	-14.5	0.56	3.54	4558	1009	811	1.3	452
	471	-12	- 8.6	-17.5	2.1	3.5	8980	3200	669	4.8	882
5/11	402	- 3.6	0	- 8.0	1.4	3.29	7160	2644	685	3.9	730
		-12.5	- 9.2	-17.0	1.3	2.89	7604	2523	632	4.0	753
		-20.8	-17.5	-27.0	1.3	2.8	8074	2606	469	5.6	778
		-29.0	-25.3	-36.0	1.4	3.08	8588	3145	516	6.0	805
7/9	241	-12.0	- - -	- - -	0.57	3.62	4558	- - -	- -	- -	452
	241	-12.0	--	- --	.99	3.53	6072	- --	--	---	603
	241	-12.0	- - -	- - -	1.5	3.47	7596	- --	- --	- --	752
7/10	241	-12.0	- 7.8	-17.8	0.61	3.86	4558	2017	364	5.6	452
	402	-12.0	- 6.9	-20.4	1.5	3.53	7596	3992	474	8.4	752
7/11	241	-12.4	- 8.6	-17.4	0.64	4.01	4563	1767	385	4.6	452
	322	-12.4	- 8.2	-17.8	1.1	3.88	6084	2590	511	5.1	603
	402	-12.4	- 7.8	-19.3	1.7	3.82	7604	3576	527	6.8	754
7/16	241	-12.4	- 7.8	-17.7	0.6	3.77	4563	2145	422	5.2	452
	402	-12.0	- 6.9	-20.8	1.5	3.47	7596	3992	448	8.9	752
8/1	241	-12.4	- 8.3	-18.8	0.53	3.37	4563	1893	311	6.1	450
8/2	443	-17.8	-12.8	-24.4	no data	no data	8694	4251	62	6.8	846
	434	-17.8	-14.4	-24.6	↓	↓	8536	2783	443	6.3	830
	434	-17.8	-15.0	-23.7			8536	2319	448	5.2	830
	121	-17.2	-13.3	-21.5			2366	900	237	3.8	230
	121	-16.7	-11.9	-22.3			2360	1091	195	5.6	230

TABLE IV. - PERFORMANCE DATA FOR IRT HEAT EXCHANGER IN SEVERE ICING CONDITIONS

Run	Airspeed, V_T, km/hr	Air temperature, °C		Freon temperature, T_F, °C	Fan speed, rpm	Fan power consumption, kW	Spray conditions			Pressure drop, ΔP_H, cm H_2O	Loss coefficient, K	Reynolds number, Re	Heat removed, Q, kW	Overall heat transfer per unit temperature of air cooled, UA, kW/°C	Log mean temperature difference, LMTD, °C	Mass flow, m, kg/sec
		T_{down}	T_{up}				Liquid water content, LWC, g/m^3	Drop size, MVD, μm	Time, min.							
5/11	402	-29.1	-25.3	-35.0	325	1750	Dry	Dry	0	1.4	3.08	8588	3145	516	6.1	805
	↓	↓	-24.7	-36.0	350	2000	0.62	12	30	2.2	4.6	8588	3595	485	7.4	805
			-24.7	-38.0	360	2150	0.62	12	60	2.8	5.95	8588	3595	390	9.3	805
			-22.7	-39.0	390	2500	0.62	12	90	3.8	8.17	8530	3794	327	11.5	800
7/10	241	-12.2	- 7.8	-18.0	230	875	Dry	Dry	0	0.61	3.86	4558	2017	364	5.6	452
	↓	↓	- 8.9	-17.0	235	900	1.36	30	7.9	.74	4.66	↓	1513	343	4.4	↓
			↓	-17.5	235	900	↓	↓	15.8	.84	5.3		↓	322	4.7	
				-18.0	240	950			23.7	1.0	6.4			295	5.1	
				-18.0	245	1000			39.4	1.1	7.2			295	5.1	
7/11	241	-12.5	- 8.6	-17.5	230	900	Dry	Dry	0	0.64	7.01	4563	1767	385	4.6	452
	↓	-12.2	- 9.3	-17.0	230	900	1.36	15	9.5	.79	4.98	4558	1311	316	4.1	↓
		↓	- 9.4	-17.8	235	950	↓	↓	19.0	.89	5.63	↓	1261	264	4.8	
			- 9.1	-17.4	245	1025			28.5	1.1	6.75		1437	316	4.5	
			- 8.9	-17.9	250	1025			39.3	1.2	7.48		1513	295	5.1	
7/16	241	-12.2	- 7.8	-17.7	225	900	Dry	Dry	0	0.6	3.78	4558	2017	379	5.3	452
	↓	↓	- 9.1	-16.7	230	900	0.5	10	19.75	.62	3.94	↓	1387	374	3.7	↓
			- 9.4	-17.0	225	----	.5	10	39.5	.7	4.42		1261	348	3.6	
			- 9.4	-17.0	---	----	.5	10	78.5	.95	6.03		1261	332	3.8	
8/1	241	-12.2	- 8.3	-18.8	200	720	Dry	Dry	0	0.53	3.38	4558	1765	279	6.3	452
	↓	↓	- 9.0	-17.0	200	---	1.92	45	9.8	.61	3.86	↓	1513	353	4.3	↓
			- 9.0	-17.0	200	800	1.92	45	19.8	.64	4.02		1513	364	4.2	
			- 9.0	-18.8	210	860	1.92	45	28.2	.65	4.1		1387	374	3.7	
8/2	241	-28.9	-24.0	-35.0	195	700	Dry	Dry	0	0.76	4.52	5147	2155	348	6.2	483
	↓	-29.0	-25.0	-37.0	230	950	1.36	15	9.75	.86	5.11	5153	1887	332	7.3	483
		-28.0	-25.0	-37.0	240	1050	1.36	15	24.5	1.0	6.2	5124	1474	332	8.4	480
		-28.0	-22.5	-38.0	270	1250	1.36	15	39.0	2.2	13.08	5124	2547	237	10.8	480

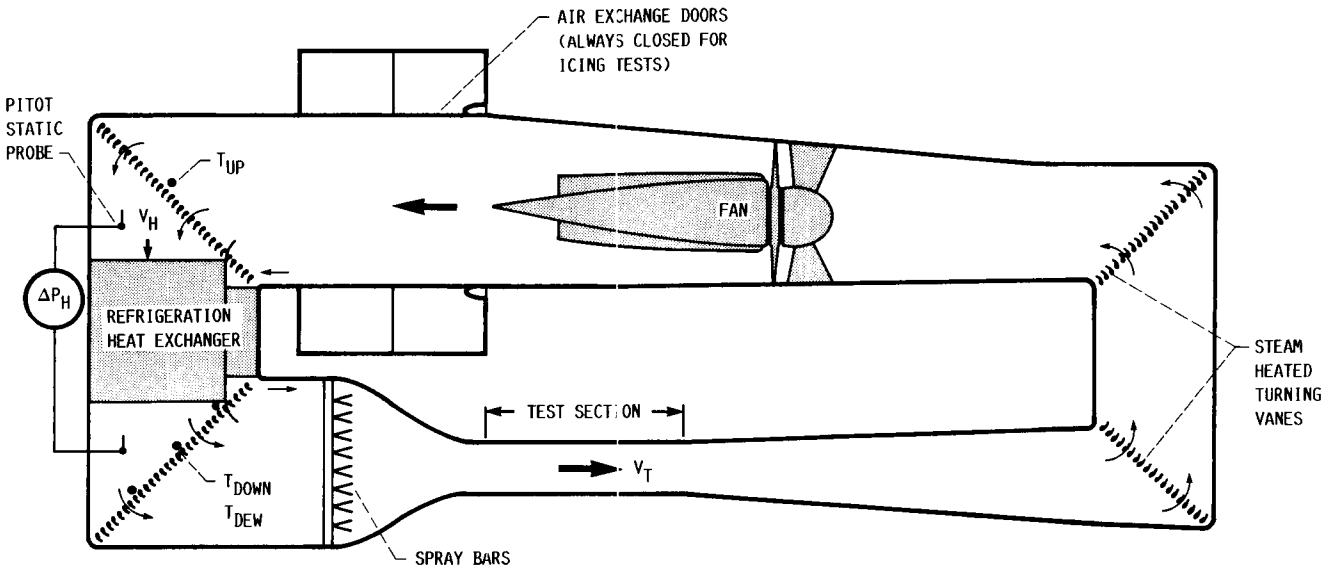

FIGURE 1. - SCHEMATIC OF ICING RESEARCH TUNNEL SHOWING INSTRUMENTATION USED IN REFRIGERATION HEAT EXCHANGER TEST.

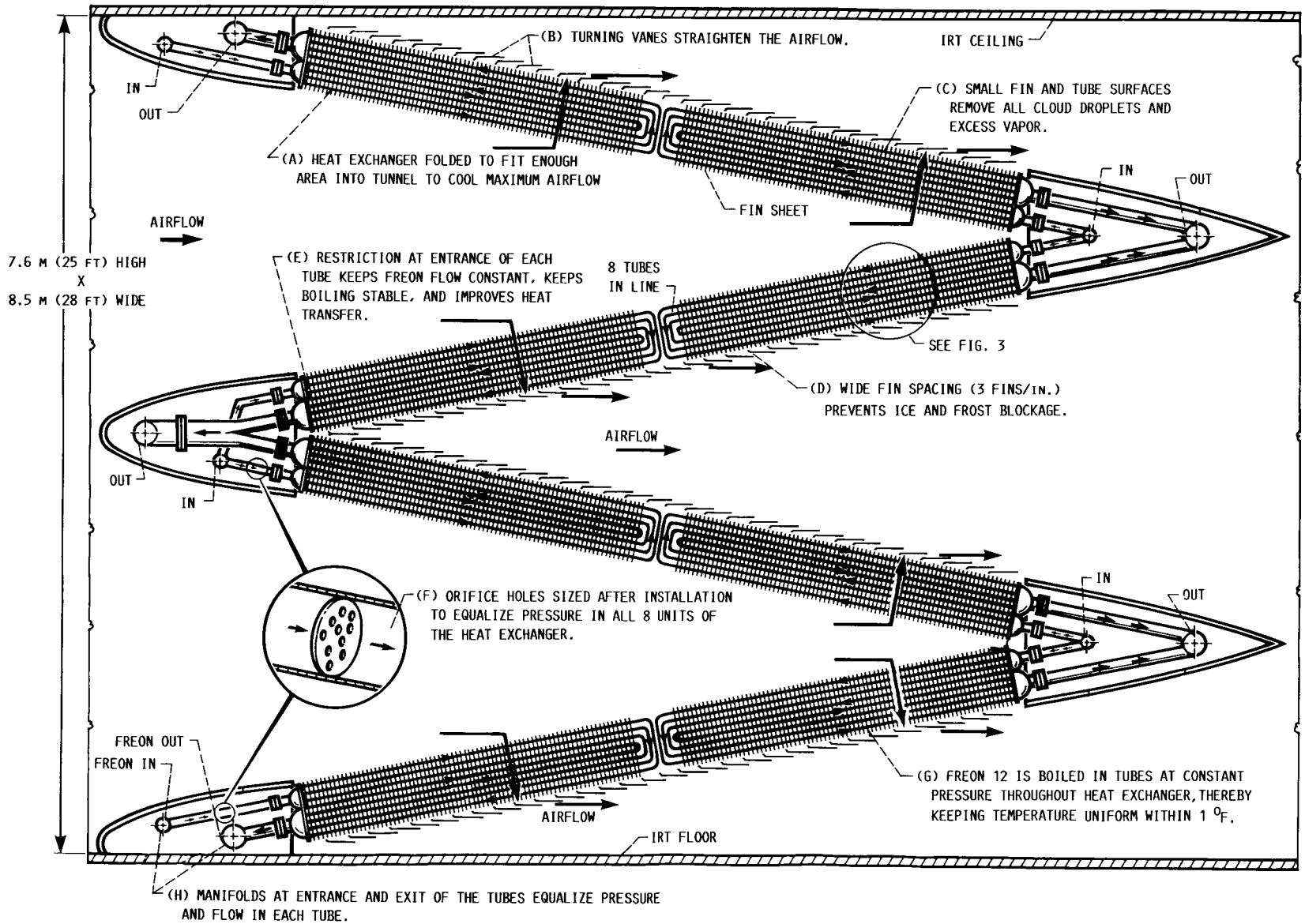

FIGURE 2. - SIDE VIEW OF THE REFRIGERATION HEAT EXCHANGER IN IRT SHOWING KEY DESIGN FEATURES A TO G THAT RESULT IN A UNIFORM AIR TEMPERATURE ACROSS TEST SECTION WITHIN ± 1/2 °C (±1 °F), EVEN UNDER SEVERE ICING CONDITIONS.

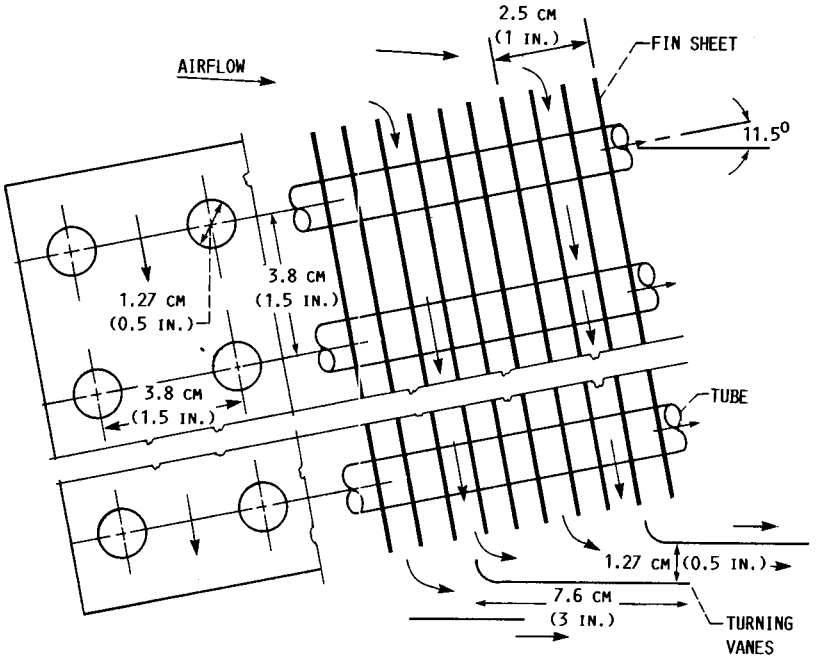

FIGURE 3. - FIN SHEETS, TUBES, AND TURNING VANES.

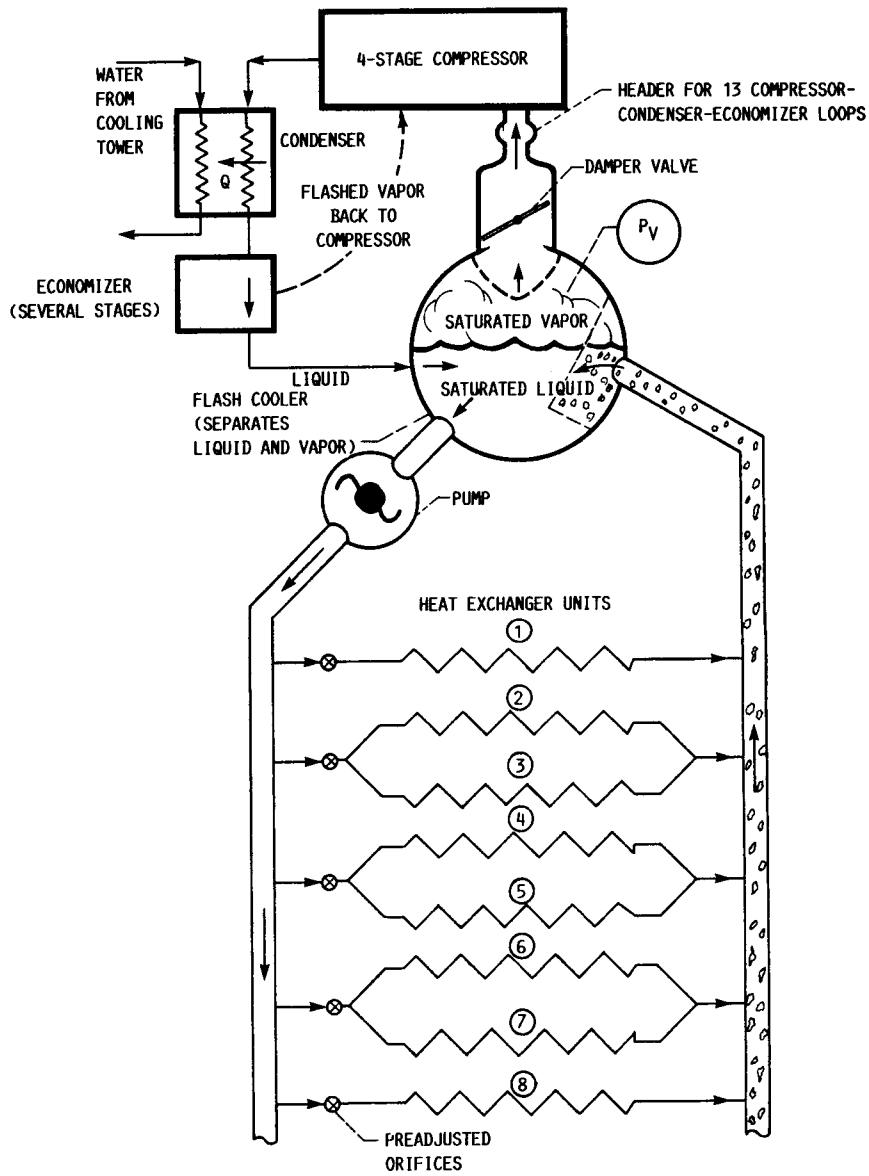

FIGURE 4. - SIMPLIFIED REFRIGERATION LOOPS.

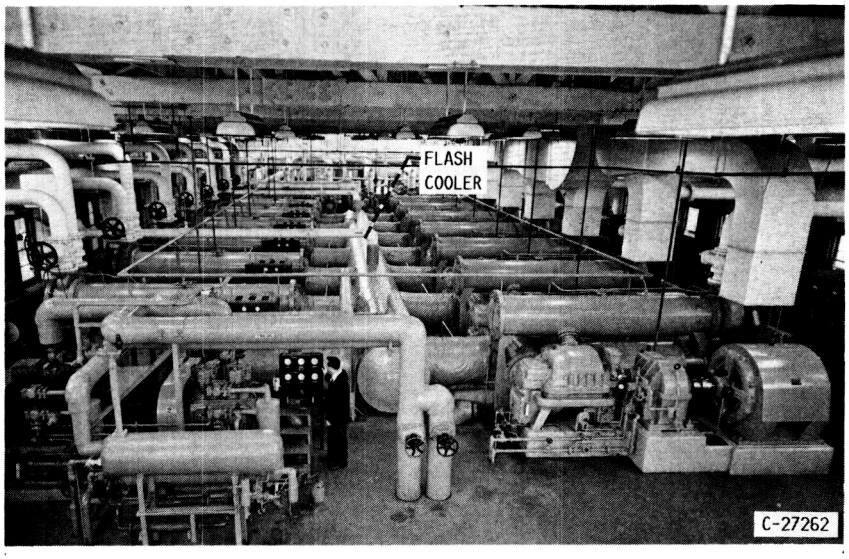

FIGURE 5. - REFRIGERATION PLANT CONSISTING OF 13 COMPRESSORS ON EITHER SIDE OF FLASH COOLER.

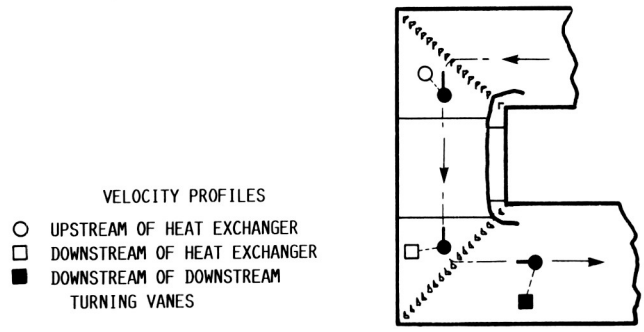

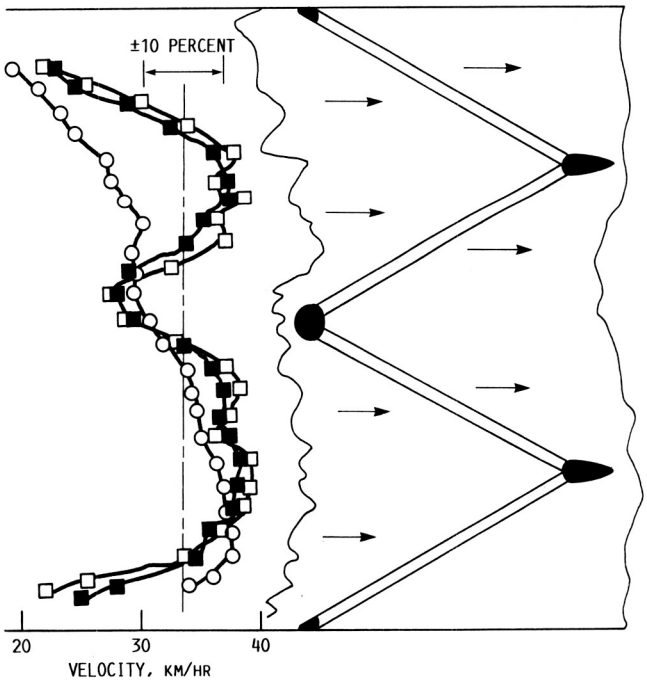

FIGURE 6. - VERTICAL CENTER-PLANE VELOCITY PROFILE UPSTREAM AND DOWNSTREAM OF THE IRT HEAT EXCHANGER. TUNNEL AIRSPEED, 402 KM/HR.

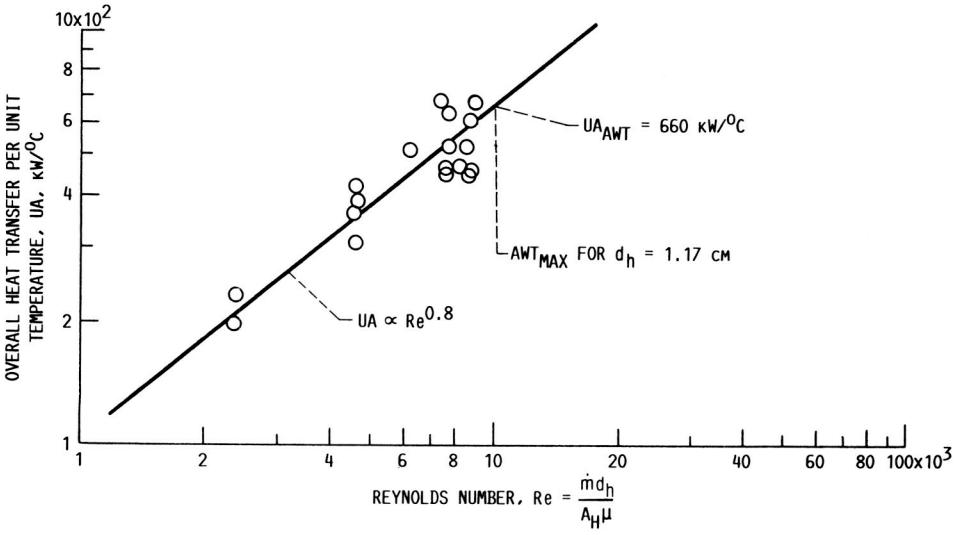

FIGURE 7. - OVERALL UA FOR DRY HEAT EXCHANGER IN THE IRT. HYDRAULIC DIAMETER OF IRT HEAT EXCHANGER FLOW PASSAGE, d_h, 1.02 cm.

FIGURE 8. - HEAT EXCHANGER AFTER ICING RUN 5/11. (OVERALL VIEW OF UNIT 1; UNITS 2 AND 3 IN BACKGROUND ARE POORLY ILLUMINATED.)

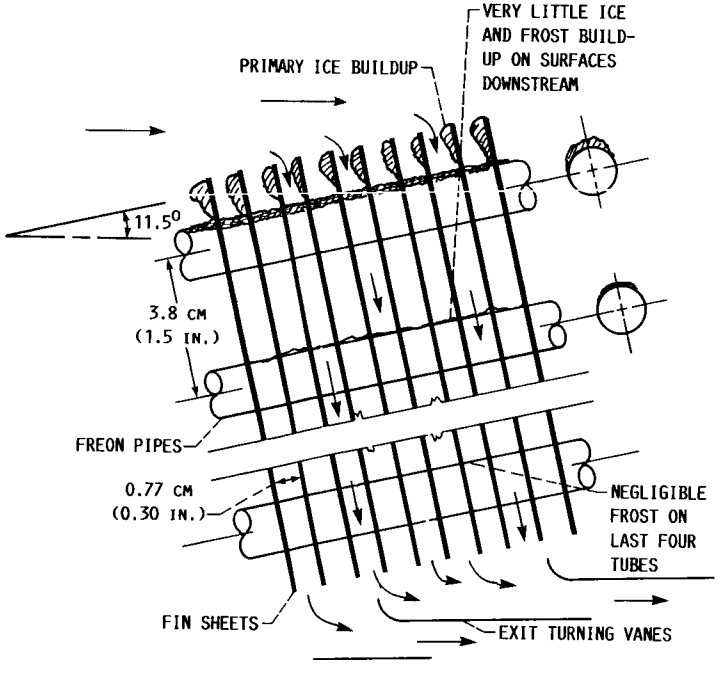

(A) RUN 5/11; CORRECTED TIME, τ_c = 70 MIN.

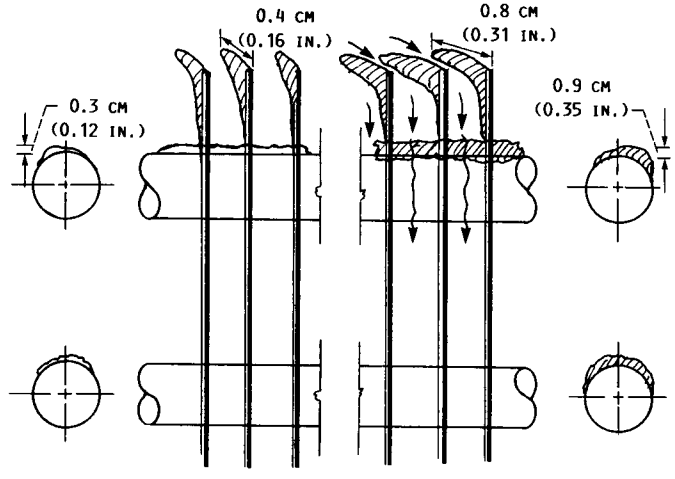

(B) RUN 7/11; CORRECTED TIME, τ_c = 39 MIN.

(C) RUN 8/1; CORRECTED TIME, τ_c = 24.5 MIN. NEARLY PLUGGED.

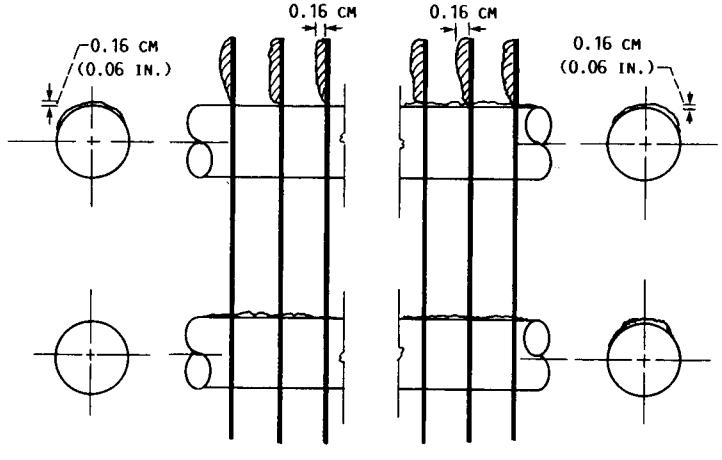

(D) RUN 8/1; CORRECTED TIME, τ_c = 23 MIN.

(E) RUN 7/10; CORRECTED TIME, τ_c = 30 MIN.

FIGURE 9. - ICE AND FROST ACCUMULATION ON REFRIGERATION HEAT EXCHANGER SURFACES FOR SEVERAL WORST-CASE ICING RUNS.

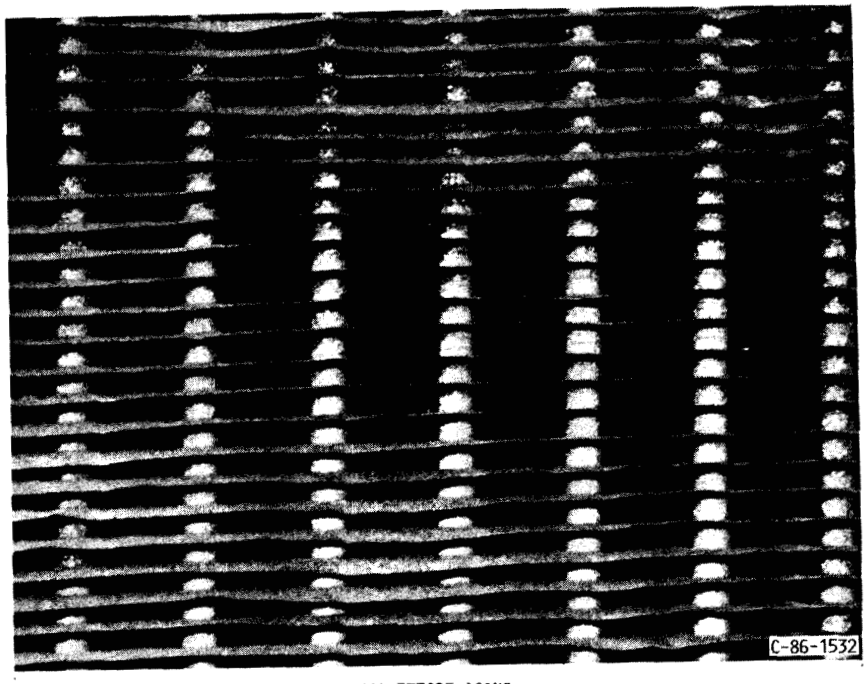

(A) BEFORE ICING.

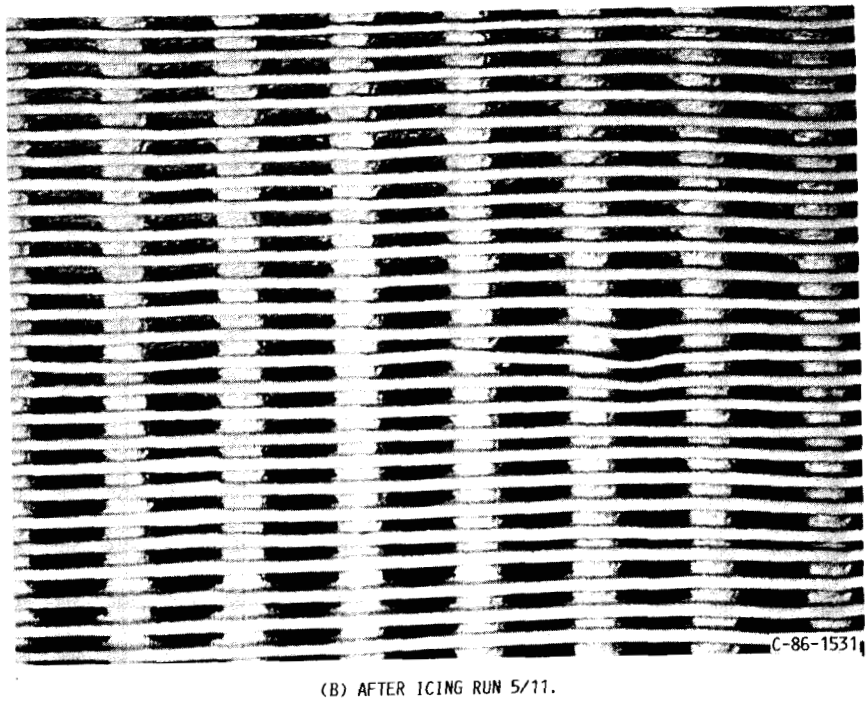

(B) AFTER ICING RUN 5/11.

FIGURE 10. - SMALL PART OF HEAT EXCHANGER FACE.

	RUN DATE	DROP-LET SIZE, d, μm	LIQUID WATER CONTENT, LWC, g/m³	AIR-SPEED, V_T, km/hr	CLOUD FRACTION REACHING HEAT EXCHANGER, X/X_{REF}	AIR TEMPER-ATURE, T_{DOWN}, °C	FROST FROM VAPOR
○	7/16	10	0.50	241	1.06	-12	LITTLE
●	5/11	12	.62	402	1.03	-29	↓
□	7/10	30	1.36	241	.76	-12	
◇	8/1	45	1.92	↓	.59	-12	
▽	7/11	15	1.36		1.00	-12	
▲	8/2	15	1.36		1.00	-29	HEAVY

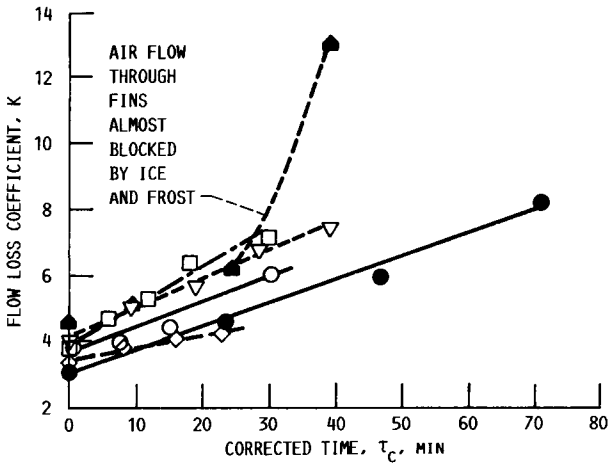

FIGURE 11. - INCREASE IN FLOW LOSS COEFFICIENT OF IRT HEAT EXCHANGER WITH TIME BECAUSE OF SEVERE ICING CONDITIONS.

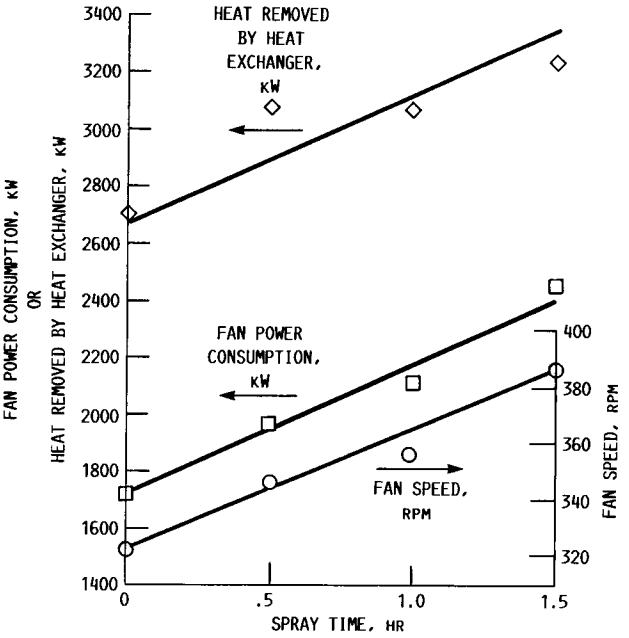

FIGURE 12. - EFFECT OF FROST AND ICE BUILDUP ON TUNNEL DRIVE FAN AND HEAT REMOVED BY HEAT EXCHANGER. RUN 5/11; CONSTANT AIRSPEED IN TEST SECTION.

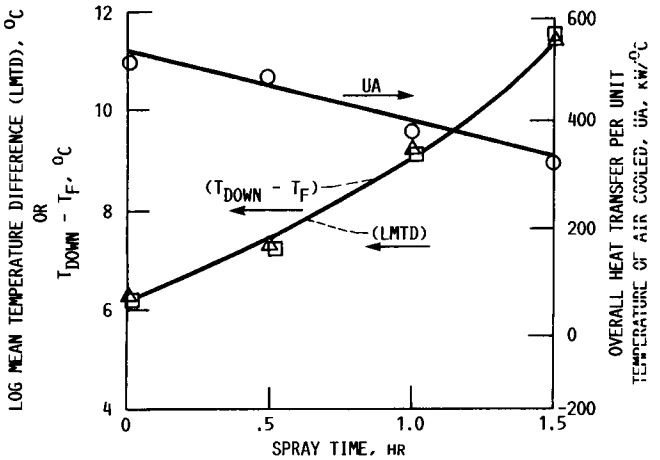

FIGURE 13. - EFFECT OF FROST AND ICE BUILDUP ON HEAT EXCHANGER THERMAL PERFORMANCE. RUN 5/11.

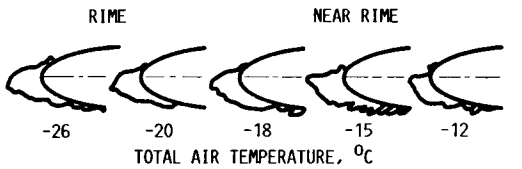

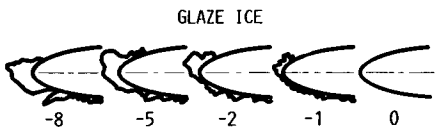

(A) ICE SHAPE.

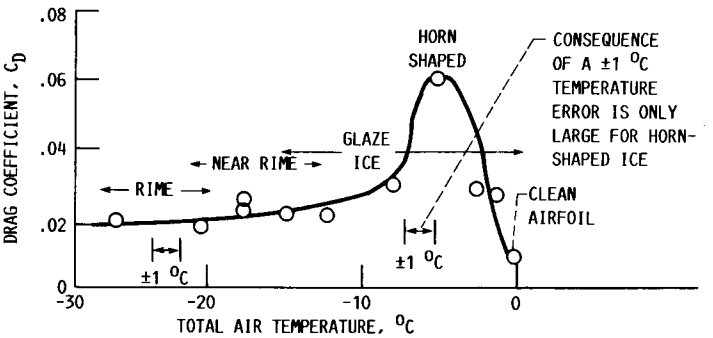

(B) DRAG COEFFICIENT.

FIGURE 14. - EFFECT OF AIR TEMPERATURE ON ICE SHAPE AND RESULTING DRAG COEFFICIENT. AIRSPEED, 209 km/hr; LWC, 1.3 g/m³; DROP SIZE, MVD, 20 μm; TIME, 8 min; AIRFOIL, 0.53-m CHORD AT 4° ANGLE.

NASA
National Aeronautics and Space Administration

Report Documentation Page

1. Report No.	2. Government Accession No.	3. Recipient's Catalog No.
NASA TM-100116		

4. Title and Subtitle	5. Report Date
Measured Performance of the Heat Exchanger in the NASA Icing Research Tunnel Under Severe Icing and Dry-Air Conditions	December 1987
	6. Performing Organization Code: 505-65-11
7. Author(s): W. Olsen, J. Van Fossen, and R. Nussle	8. Performing Organization Report No.: E-3661
	10. Work Unit No.
9. Performing Organization Name and Address: National Aeronautics and Space Administration, Lewis Research Center, Cleveland, Ohio 44135	11. Contract or Grant No.
	13. Type of Report and Period Covered: Technical Memorandum
12. Sponsoring Agency Name and Address: National Aeronautics and Space Administration, Washington, D.C. 20546	14. Sponsoring Agency Code

15. Supplementary Notes

16. Abstract

Measurements were made of the pressure drop and thermal performance of the unique refrigeration heat exchanger in the NASA Lewis Icing Research Tunnel (IRT) under severe icing and frosting conditions and also with dry air. This information will be useful to those planning to use or extend the capability of the IRT and other icing facilities (e.g., the Altitude Wind Tunnel (AWT)). The IRT heat exchanger and refrigeration system is able to cool the air passing through the test section down to at least a total temperature of -30 °C (well below the requirements of icing), and usually up to -2 °C. The system maintains a uniform temperature across the test section at all airspeeds. Holding a uniform temperature is more difficult and time consuming at low airspeeds, at high temperatures, and on hot humid days when the cooling towers are less efficient. Tests show that the very small surfaces of the heat exchanger prevent any icing cloud droplets from passing through it and going through the test section again. The original designers of the IRT designed the heat exchanger that would not be adversely affected by severe icing. During a worst-case icing test the heat exchanger iced up uniformly enough so that the temperature uniformity was no worse than about ±1 °C. The overall conclusion is that the IRT heat exchanger, which was designed and built more than 40 years ago, is a sophisticated unique design that performs superbly and is necessary for icing research.

17. Key Words (Suggested by Author(s))	18. Distribution Statement
Icing Heat exchanger	Unclassified - Unlimited Subject Category 37

19. Security Classif. (of this report)	20. Security Classif. (of this page)	21. No of pages	22. Price*
Unclassified	Unclassified	28	A03

NASA FORM 1626 OCT 86

*For sale by the National Technical Information Service, Springfield, Virginia 22161